Available online at www.sciencedirect.com
SCIENCE DIRECT®
Journal of Electron Spectroscopy and Related Phenomena 148 (2005) 107–114
JOURNAL OF ELECTRON SPECTROSCOPY and Related Phenomena
www.elsevier.com/locate/elspec

Electron-induced KLL Auger electron spectroscopy of Fe, Cu and Ge

M.R. Went*, M. Vos

Atomic and Molecular Physics Laboratory, Research School of Physical Sciences and Engineering, The Australian National University, Canberra 0200, Australia

Received 27 January 2005; received in revised form 31 March 2005; accepted 8 April 2005
Available online 23 May 2005

Abstract

KLL Auger spectra excited by electrons with energies in the 30–35 keV range of Fe, Cu and Ge films were measured, using thin free-standing films. It was possible to obtain spectra with an energy resolution of about 1 eV. The observed spectra can *not* be described satisfactorily by just the multiplet splitting of the final state as calculated for an isolated atom. Additional features, due in part to intrinsic (shake satellites) and in part to extrinsic (energy loss of the escaping electron) processes formed a large fraction on the observed intensities. In particular a number of distinct satellite structures that are not predicted by the atomic Auger process are observed. For Fe and Cu the satellite peaks can be explained in terms of shake-up processes from the $3d_{5/2}$–$4d_{5/2}$ states. Similar satellite structures observed in Ge are partly attributed to plasmon creation and partly to shake-up processes. It is demonstrated that both the thickness dependence of the observed intensity distributions and transmission electron energy loss measurements contain invaluable information for the interpretation of these spectra.

PACS: 79.20.Fv; 32.80.Hd

Keywords: KLL Auger spectra; Electron excitation

1. Introduction

Quantitative understanding of the behaviour of energetic electrons in matter is essential for interpreting a variety of experimental techniques such as photoemission and electron microscopy. Recent advances in synchrotron technology has meant that high-energy XPS (5–10 keV) experiments are a reality [1]. These experiments are supposed to be bulk sensitive and their interpretation should be relatively simple as surface effects are small. One process that contributes to the XPS spectra in this energy range is the KLL Auger electron spectra of the 3d elements. From atomic physics we know that these Auger spectra display a multiplet structure. For elements with $18 \lesssim Z \lesssim 35$ the multiplet structure is not well described in either the non-relativistic LS coupling scheme or the relativistic jj coupling scheme and an intermediate coupling scheme has to be applied [2]. In recent years relatively high-resolution spectra of these KLL Auger transition have become available. However, the interpretation has turned out to be less than straightforward. Here we use a somewhat different approach to measure these spectra (electron induced Auger spectra from thin, free-standing films) and see if these data can contribute to a quantitative understanding of the spectra.

There are two limiting factors that restrict the use of KLL Auger spectroscopy for heavy elements. The first limiting factor is the increasing fluorescence yield with increasing Z. Going from $Z = 20$ to $Z = 40$ the fluorescence yield increases from 20% to 80% and hence the Auger yield will decrease in a complementary way [3,4]. At the same time the lifetime of the K level decreases with increasing Z [4–6]. For example, the lifetime broadening is calculated to be 1.1, 1.6 and 2.5 eV for $Z = 25$, 30 and 35, respectively[4]. This sets a clear lower limit for the line width one can expect for KLL Auger lines. Thus the KLL Auger line of the third row of the periodic table provides a series of tests of our understanding of keV electrons with reasonable sharp structures and high intensity.

* Corresponding author.
E-mail address: michael.went@anu.edu.au (M.R. Went).
URL: http://rsphysse.anu.edu.au/ampl/research/ems/.

0368-2048/$ – see front matter © 2005 Elsevier B.V. All rights reserved.
doi:10.1016/j.elspec.2005.04.004

Over the last few decades KLL Auger measurements have become available with higher and higher resolution. It turns out that the spectra obtained for *solids* display more structure than that predicted by theory based on KLL Auger decay of *isolated atoms*. It is this difference that is of interest. It is due to the response of the solid on the new final state created (*intrinsic* effects), and due to energy loss of the Auger electrons before they leave the film (*extrinsic* effects). Understanding of these effects is important for all electron spectroscopies using keV electrons. In this paper we investigate if electron-induced Auger spectra of thin films can be of help in addressing these questions.

While only a few authors [7–9] have investigated the KLL spectra of Fe it is clear that the atomic multiplet structure is resolved [2,4,10,11] in these spectra, but the multiplet structure by itself fails to describe quantitatively the observed intensity distribution. In addition the for-mentioned intrinsic and extrinsic loss processes play an important role. In the case of Fe they produce a large asymmetric line shape for each multiplet and an additional peak (satellite) was observed in the recent work [9].

The earliest investigation of Cu was by Asaad and Burhop [12] who measured the relative energies of the $^1S_0$ and $^3P_2$ peaks. Sokolowski and Nordling [13] concurrently detected a satellite to the main $^1D_2$ line. The satellite was attributed to contributions from inelastic scattering. However, the sharp nature of this satellite and the lack of any corresponding features in the electron energy loss spectra [14] indicated that this is not the case. Kövér et al. [15] recently attributed the peak to 3d spectator vacancy shake-up processes, similar to those observed in the X-ray excited LMM Auger spectra of Ag [16]. Kövér et al. [15], however, gave no indication as to why similar satellites were not observed for the other lines of the spectra. Cserny et al. [17], using molecular orbital calculations predicted the position of this satellite which was highly dependent on the amount of screening of the core hole. With more recent measurements [18], they found a second satellite below the $^1S_0$ line and calculated the intensity of the earlier observed satellite. The presence of these satellites in Cu means that calculations based on atomic physics [4,11] alone fail to describe spectra obtained from solids.

Ge is the least studied among the three elements presented here. Only two experimenters investigated this target prior to this work [19,20]. As for the theoretical side, Chen et al. [11,4] calculated the relative intensities of a range of targets, $13 \leqslant Z \leqslant 96$, and Larkins [2] reported the semi-empirical calculations. Kovalík et al. [19] measured the AES of Ge using the internal conversion method with an experimental resolution of 7 eV, missed the satellite structure observed recently by Berényi et al. [20]. The satellites observed in Ge have been attributed partly to intense plasmon losses and partly to "shake-up" processes [20].

Thus the interpretation of these KLL Auger spectra still provides a significant challenge for experimenters and theorists as solid state effects complicate the Auger spectra. The structure due to inelastic scattering (e.g. plasmon loss) needs to be considered for a full understanding of the resulting Auger spectra. In some cases these spectra show satellites that cannot be explained by extrinsic processes alone. But in the case of copper, for example, the calculated intensity and observed intensity of the intrinsic satellites differ by almost an order of magnitude [18].

These measurements depend on the core hole production in the deep K-shell. The initial Auger measurements used nuclear decay by internal conversion electrons to create the core hole [21]. Nowadays copper Kα radiation is used for elements lighter than Cu and Bremstrahlung for heavier elements. Some data were obtained using monochromatized copper Kα [22] radiation or by synchrotron radiation [10]. In this work we wish to demonstrate that, provided one uses thin free-standing films, KLL Auger spectroscopy at keV energies can be performed using electrons to produce the deep core holes. Thus there is no requirement of a hard X-ray source and this approach eliminates spurious photoelectron peaks that sometimes contribute to the measured distributions. However electron induced Auger spectra are subject the same intrinsic and extrinsic processes observed in X-ray induced Auger electron spectroscopy or AES produced by internal conversion/electron capture processes.

In this paper we present the electron-induced KLL Auger spectra for Fe, Cu and Ge and compare these measurements with the available experiments and theoretical calculations and discuss the nature and origin of extrinsic and intrinsic processes observed in the Auger spectra of Fe, Cu and Ge.

2. Experimental

2.1. Spectrometer description

The Auger measurements were done using the electron momentum spectrometer of the Australian National University [23] (see Fig. 1) and only details pertaining to these measurements will be discussed here. An electron gun produces a 25 keV beam which impinges on a sample held at an energy (E_A) close to that of the Auger transition of interest. Thus electrons with energy $E_A + 25$ keV strike the target which corresponds to 3–4× the K-shell ionization energy. This is close to the energy at which the K-shell ionization cross section has its maximum [24]. Auger electrons emitted from the target at ≈45° to the incident beam direction, enter a lens system which decelerates and focuses the electron at the entrance plane of a hemispherical analyzer with a pass energy of 400 eV. Electrons are dispersed as they pass through the hemisphere and are detected on a two dimensional position sensitive detector, mounted at the exit of the spectrometer. This configuration allows the simultaneous collection of a range of energies and over a 13° azimuthal angle.

Electron energy loss spectroscopy (EELS) measurements, used for background removal in Ge, were also performed using this apparatus. In this case the electron gun and analyzers were held close to ground while the sample was set at the

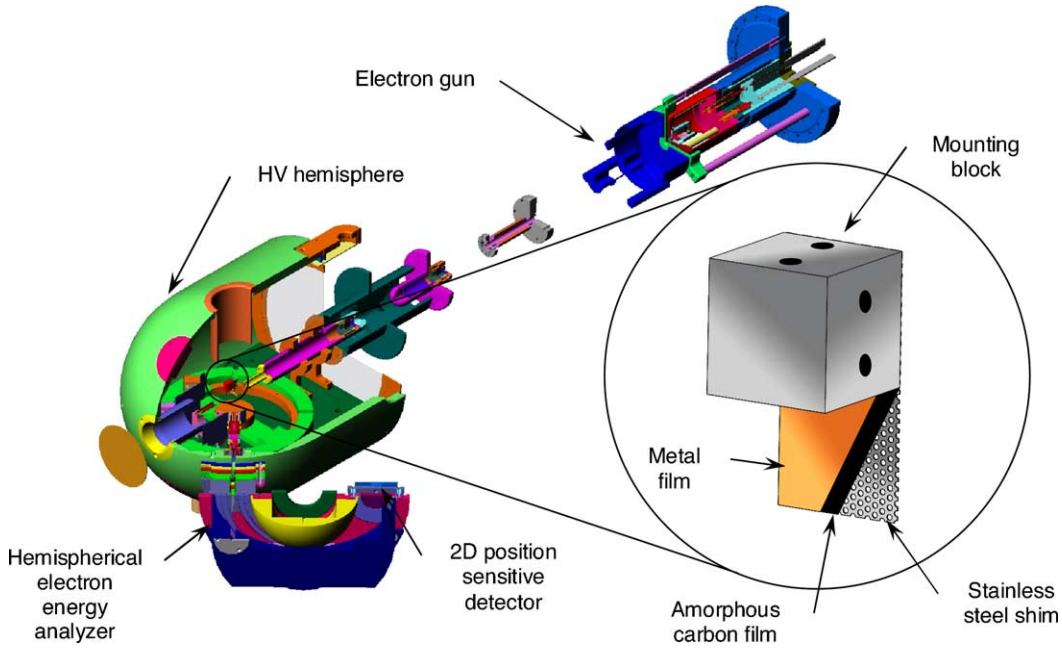

Fig. 1. Schematic representation of the spectrometer.

energy of the Auger transition (E_A). Thus electrons emitted from the gun strike the sample with energy E_A and elastically scattered electrons are decelerated and focused into the spectrometer. By varying slightly the analyzer float potential a range of energies can be scanned across allowing EELS spectra to be measured. From the elastic peak obtained under these conditions we obtain the analyzer energy resolution. The total energy resolution of the Auger experiment is estimated to be 1 eV resulting from the intrinsic resolution of the analyzer (0.6 eV), a high frequency ripple on the high voltage power supply (0.1 eV) and a typical drift over a measurement period (0.3 eV).

2.2. Sample preparation

Due to the transmission nature of our experiment the samples need to be self supported and thin (≈10 nm). For this purpose, we use the same sample preparation methods as for electron momentum spectroscopy experiments. A thin 3 nm amorphous carbon film is floated off a glass slide on which it is mounted using de-ionized water. The film is then lifted onto a regular array of 0.3 mm diameter holes in a stainless steel shim. The shim is mounted on a stainless steel block used to transport the samples in vacuum (Fig. 1). After drying the sample is loaded into vacuum via a load lock and the films are annealed using electron bombardment to remove contaminants and thinned further by using an argon ion sputter gun.

The samples are then introduced into the evaporation chamber where various metallic samples can be evaporated using either an e-beam evaporator or resistive heater evaporator. The base pressure in this chamber is the order of 10^{-8} Torr during the evaporation. The Fe and Cu samples were prepared by e-beam evaporation of metal rod targets while the Ge samples were prepared by resistive heating of a tantalum boat containing the Ge metal. Ten-nanometer thick metallic films were deposited onto the carbon films by this method (Fig. 1). The thickness of the evaporated films was determined with a crystal thickness monitor. During the actual experiment the transmitted electron beam is monitored on a phosphorous screen. The diffraction patterns observed correspond to those of polycrystalline iron (bcc) and copper (fcc), whereas that of germanium was typical for an amorphous target, lacking sharp diffraction rings.

2.3. Experimental procedure

After a sample is evaporated, it is moved to the main spectrometer chamber for the Auger measurement. This transfer is completed entirely under ultra high vacuum to ensure sample quality is maintained. In the main chamber one of the 0.3 mm diameter samples is aligned with the incident electron beam with the carbon side closest the incoming beam. Most of the electron beam is transmitted through the 13 nm thick C-metal sandwich structure and dumped in a Faraday cup. In a thin free-standing film the incoming electrons are unlikely to lose most of their energy *and* be deflected over 45°. Thus using a thin free-standing target we can obtain electron-induced Auger spectra on a relatively low background. A typical measurement is performed over two days with the operating pressure in the main chamber better than 2×10^{-10} Torr. No significant deterioration of the sample was observed in these bulk-sensitive measurements.

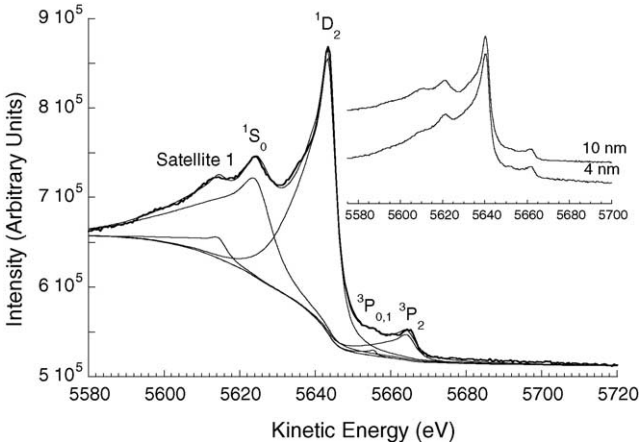

Fig. 2. Electron excited Fe KLL spectra from thin self-supporting metallic samples of ≈10 nm thickness. Figure shows asymmetric line shape deconvolution on top of a Shirley type background. The inset shows a comparison of the Auger spectra for 10 and 4 nm thick films.

3. Results and discussion

3.1. Iron

In Fig. 2 we present the $KL_{23}L_{23}$ Auger spectra as measured for a 10 nm thick film. The $^1S_0$, $^1D_2$ line and $^3P_2$ line are clearly observed for both films. Additional peak just above the $^1D_2$ line may indicate the presence of the $^3P_{1,0}$ line but its intensity is too small to be analyzed quantitatively. Another structure is clearly resolved at 5614.2 eV. This peak is referred to as satellite 1 in Table 1 and Fig. 2. It has been observed previously [9] and identified as a plasmon loss feature. However the observed position and shape do not correspond to the peak in the Fe EELS spectra, which show a broad maximum at an energy loss value of ≈22 eV [14]. This suggests the presence of additional "shake-up" processes, such as those observed in Cu [17,18,25]. Coster-Kronig processes, often the origin of intensity at the low kinetic energy part of L_3VV Auger spectra do not occur for KLL Auger spectra.

The intensity at the low energy side remains higher than that at the high energy side. The asymmetric distribution was also observed in the previous measurements [8,9]. Thus, asymmetric peak shapes were chosen for fitting to the measured spectra, while background removal is done using the Shirley algorithm [26]. It was found that strongly asymmetric peaks were required for all components in order to get a reasonable fitting. Peak positions were determined in this way and were compared with the literature values in Table 1. However, no meaningful data could be obtained on the relative intensity of the peak because this depends completely on the asymmetry of the line shape used in the fitting procedure. In ref. [9] reasonable agreement was found between calculated and measured relative intensities using a very asymmetric line shape for each multiplet, but, for example, areas obtained from the fitting procedure shown in Fig. 2 are completely different. It is thus very difficult to compare, for iron, observed intensities with the calculated multiplet intensities.

To get some insight in the origin of the asymmetric line shape we studied a 4 nm thick Fe film as well. A comparison between the 4 and 10 nm results is shown as an inset in Fig. 2. The asymmetry of the line shape is reduced in the spectrum of the 4 nm film. This means that at least a large part of the asymmetry is due to extrinsic effects. Thus, for satisfactory fitting, it is required to consider the thickness dependence. Electron spectroscopy data for iron are known to have a much larger step in the background compared to other elements [27]. Hence analysis of the copper and germanium data (to be shown next) is significantly less affected by this problem.

The relative peak energies presented in Table 1 show good agreement with previous experiments with the exception of the $^1S_0$ line, measurement of Kovalík et al. [8], which lies lower than ours by more than 2σ. This difference was also observed by Némethy et al. [9]. Comparison with the theoretical relative energies indicates that the size of the multiplet splitting is calculated with a precision of 10%.

3.2. Copper

In Fig. 3 we present the electron excited AES of Cu. We can clearly see that the peak asymmetry is reduced compared to Fe and that the width of the $^1D_2$ line is smaller. Thus the Auger spectrum is sharper in spite of the fact that the lifetime broadening is expected to increase with increasing Z. Besides the multiplet structure we observe two additional 'satellites': one below the main $^1D_2$ line and another satellite below the $^1S_0$ line. The line nearer the $^1D_2$ ('satellite 2') line was originally attributed to inelastic loss mechanisms [13] but the lack of a strong corresponding feature at 11.6 eV energy loss in the EELS spectra [14] makes this doubtful.

Recently the structure observed in the Cu KLL AES was attributed to "shake-up" satellites ($3d_{5/2}$–$4d_{5/2}$) in both the initial and final states [18] but no explanation was given as to why these structures were not observed in the other lines.

Table 1
Fe KLL energies relative to the $^1D_2$ line and KL_3L_3 ($^1D_2$) transition energy (eV): (T)heory and (E)xperiment

Line	This work	Ref. [9] (E)	Ref. [8] (E)	Ref. [10] (*a*) (T)	Ref. [10] (*b*) (T)	Ref. [2] (T)
Satellite	−29.2(1)	–	–	–	–	–
KL_2L_2 ($^1S_0$)	−19.3(1)	−19.8(0.5)	−24.0(2)	−21.4	−18.2	−17.8
KL_3L_3 ($^3P_{1,0}$)	–	–	–	10.0, 10.8	9.9, 11.8	10.1, 11.0
KL_3L_3 ($^3P_2$)	20.8(0.5)	21.8(0.5)	21(9)	20.1	20.6	20.3
$E(^1D_2)$	5643.4	5640.6(0.8)	–	–	–	5624.8

Quoted errors are estimates of one standard deviation.

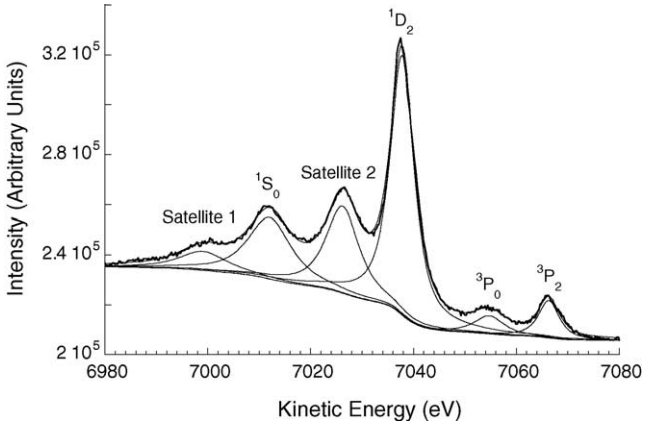

Fig. 3. Electron excited Cu KLL spectra from thin self-supporting metallic samples of ≈10 nm thickness. Figure shows line shape deconvolution on top of a Shirley type background, analyzed assuming four multiplets ($^1S_0$, $^1D_2$, $^3P_0$ and $^3P_2$) and two satellites (Model 1).

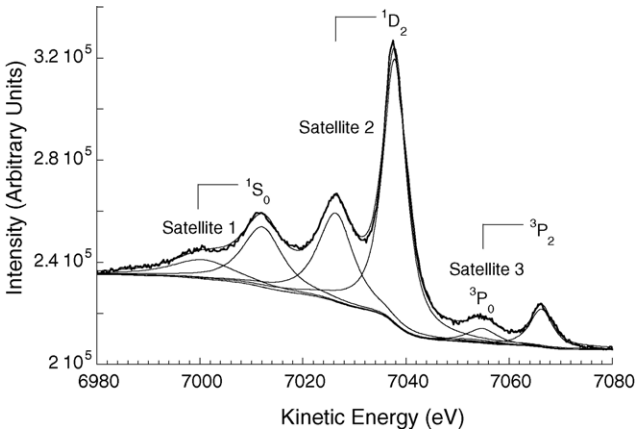

Fig. 4. Electron excited Cu KLL spectra from thin self-supporting metallic samples of ≈10 nm thickness. Figure shows line shape deconvolution on top of a Shirley type background, analyzed assuming an identical satellite structure for each of the $^1S_0$, $^1D_2$ and $^3P_2$ peaks (Model 2).

At present only the molecular orbital theory of Cserny et al. [17] predicts the position of this satellite. They found that the position of this satellite is dependent on the amount of screening of the core holes which varies from −15.8 eV for an unscreened hole, to −10.5 eV for a screened hole, suggesting the importance of screening in Cu [17]. The lack of other theoretical calculations which predict this phenomenon suggests that a complete theoretical description has not yet been achieved. In this work we present two models. The first is that that all peaks observed are independent (Model 1, Fig. 3). The second one is that *each* multiplet produces a satellite at lower energy separated by −11.44 eV and with an intensity half that of the parent multiplet. The position and intensity of the satellite are determined empirically, but position is in the range of values calculated by Cserny et al. [17] but its intensity is much larger [18]. Using these constraints we get very good agreement with a pseudo-Voigt peak fit to the observed structure (Fig. 4).

The relative energies obtained with Model 1 is given in Table 2, while the relative energies with Model 2 are not given because the multiplet peak positions were virtually identical to those obtained by Model 1, and there are no additional adjustable parameters. We find excellent agreement between these measurements and those performed previously [18]. The agreement with the theory is reasonable, the most notable difference is in the energy of the $^1D_2$ line which Larkins [2] calculates for an isolated atom to be 7 eV lower than that observed in a solid. More importantly is the lack of calculations that predict the presence of such intense satellites.

In Table 3 we present the relative intensities of the observed lines under both models and the full width half maximum under Model 1. There are large discrepancies between these measurements and those of Kövér et al. [18] and are in part due to allowing a varying width in our analysis, and in part due to the differences in the background removal technique to which intensity measurements are particularly sensitive. The main differences between our measurements and the previous experiment [18] is in the region below the $^1D_2$ peak where inelastic scattering of the $^1D_2$ Auger electrons begin to contribute. This difference is highlighted in the region between the $^1S_0$ line and satellite 2 where the modified Tougaard background [18] reduces the intensity to zero in contrast to what we determined and to the measurements in a later paper [25] both of which find non-zero intensity in this region.

3.3. Germanium

Measurements of the AES of Ge are given in Fig. 5 for thickness of 10 nm. We can see that, besides the multiplet structure, a very large satellite structure is visible in the spectrum. All of the main Auger lines are clearly resolved and have a small FWHM (listed in Table 4) marginally sharper

Table 2
Cu KLL energies relative to the $^1D_2$ line and KL_2L_3 ($^1D_2$) transition energy (eV): (T)heory and (E)xperiment

Line	This work (Model 1)	Ref. [18] (E)	Ref. [2] (T)	Ref. [12] (T)	Ref. [17](T)
Satellite 1	−38.8(1.0)	−39 (1.5)	–	–	–
KL_2L_2 ($^1S_0$)	−25.8(0.5)	−26.0(1.0)	−24.2	−29	–
Satellite 2	−11.6(0.5)	−11.3(0.5)	–	–	−10.9
KL_3L_3 ($^3P_0$)	17.0(1.0)	15.9(1.0)	16.3	–	–
KL_3L_3 ($^3P_2$)	28.5(0.5)	28.7(0.5)	26.6	26	–
$E(^1D_2)$	7037.8	7038.2(0.5)	7031.1	–	–

Quoted errors are estimates of one standard deviation.

Table 3
Cu KLL intensities relative to the KL_2L_3 ($^1D_2$) line (%): (T)heory and (E)xperiment

Line	This work FWHM (eV) (Model 1)	This work intensity (Model 1)	This work intensity (Model 2)	Ref. [18] (E)	Ref. [4] (T)	Ref. [11] (T)	Ref. [18] (T)
Satellite1	11.1	15	19	6 (1)	–	–	–
KL_2L_2 ($^1S_0$)	10.0	42	38	17 (1)	9	9	–
Satellite 2	7.7	47	50	22 (+7)	–	–	3.4
KL_2L_3($^1D_2$)	5.6	100	100	100	100	100	100
KL_3L_3 ($^3P_0$)	6.9	9	3	5 (1)	4	3	–
Satellite 3	–	–	6.5	–	–	–	–
KL_3L_3 ($^3P_2$)	4.8	12	13	14	15	16	–

Quoted errors are estimates of one standard deviation.

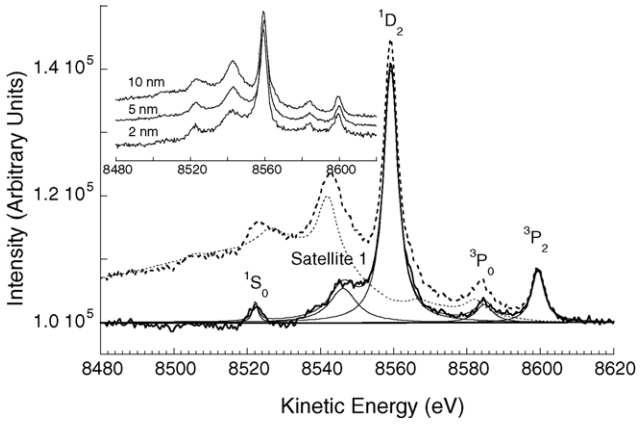

Fig. 5. Electron excited Ge KLL spectra from thin self-supporting metallic samples of ≈10 nm thickness. Figure shows raw spectra (dashed line), background convoluted from EELS spectra (dotted line), background removed (solid line), pseudo Voight fit (thin line). Insert shows a comparison of the raw Auger spectra for 10, 5 and 2 nm thick films.

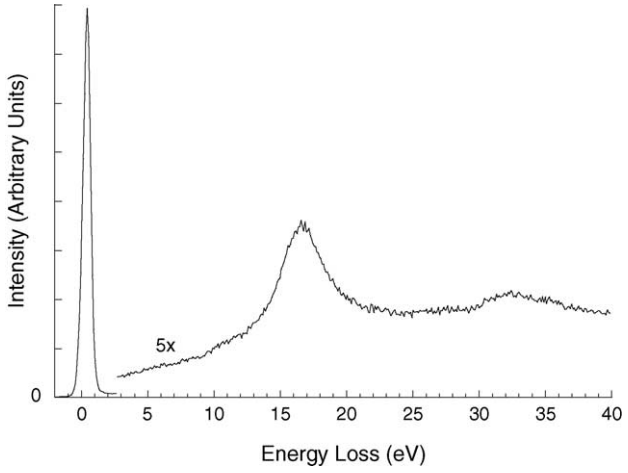

Fig. 6. Electron energy loss spectra for 10 nm thick Ge films.

than the FWHM in Cu. A large part of the satellite intensity is due to well-defined plasmon peak in the EELS spectra (Fig. 6). The extrinsic nature of (at least a part of the intensity of) the satellite is confirmed by the thickness dependence of the shape of the Auger spectra as shown in the inset of Fig. 5 for samples of a thickness of 10, 5 and 2 nm. Early measurements of the KLL AES of Ge using a thin radioactive source [19] had a relatively poor (7 eV) energy resolution and did not resolve these satellites but instead attributed the additional intensity to inelastic scattering. More recently [20] these satellite structures were resolved and were attributed to a combination of plasmon losses and shake processes.

The measurements performed in this work confirm the origin of part of these satellites as due to plasmon losses. As such, the simple Shirley model used for background correction would be inadequate for this element. We implemented the Tougaard-like [28] model as described in Berényi et al. [20] to remove the inelastic background and plasmon peaks. The EELS spectra measured was fitted with a combination of the "universal inelastic cross section" [29] and Lorentzian peaks for each of the plasmon loss peaks. Deconvolution was performed such that the background on the low energy side of the spectra was reduced to zero. This corresponds closely to removing the same amount of inelastic scattering as that determined from the EELS spectra despite the fact that the paths taken by the electrons in the Auger and EELS process are

Table 4
Ge KLL energies (eV) and intensities (%) relative to the KL_2L_3 ($^1D_2$) line

Line	Relative energy (eV)			Relative intensity (%)				
	This work	Ref. [19] (E)	Ref. [2] (T)	FWHM	This work	Ref. [19] (E)	Ref. [11] (T)	Ref. [4] (T)
$^1S_0$	−36.9(1)	−38.8(8)	−34.8	2	3	7.8(6)	8.4	6.2
Satellite 1	−13.0(2)	–	–	9	25	–	–	–
$^1D_2$	0	0	0	5	100	100	100	100
$^3P_0$	25.5(1)	24.6(7)	24.8	6	8	5.4(4)	4.6	3.7
$^3P_2$	40.2(0.5)	40.7(4)	38.9	4	18	18.5(4)	18.6	21.2
$E(^1D_2)$	8559.2	8567.4(11)	8561.5	–	–	–	–	–

Quoted errors are estimates of one standard deviation.

of different lengths (the "average" Auger electron originates halfway across the film, whereas the EELS electrons transverse the complete film). After deconvolution of the EELS spectra from the AES the resulting source function was fitted with a number of Lorentzian peaks which were used to determine the relative position and intensity of the Auger lines. The deconvolution has a major effect on the intensity and position of the $^1S_0$ component. Measurements of the thinnest 2 nm thick films indicated that there was another contribution to the background. The intensity of the background at low energies is lower than that at high energies a result which is un-physical (see inset of Fig. 5). As the signal to background is poorest for the 2 nm thick film, it is thought that this component is a combination of contributions from the amorphous carbon (3 nm thick) film and a reduced transmission of the electron energy analyzer at lower energies. These problems are less significant for thicker films as the signal to background is considerably higher and the signal from the metal film dominates that of the carbon.

The measurements of the relative energies and intensities for Ge are given in Table 4. For the relative energies there is reasonable agreement between our measurements, those of the other experimenters and between the semi-empirical theory of Larkins [2]. The measurement of the $^1S_0$ line was determined to be 2 eV higher than the previous measurement [19] and 2 eV lower than the calculated energy [2]. Similar differences are observed for Cu and Fe when compared to the theory [2]. The difference between the two experiments is likely due to the poorer energy resolution of the earlier work (7 eV). For the relative intensities there is significant discrepancies between these measurements and those of Kovalík et al. [19] these differences are greatest at energies below the $^1D_2$ line where the contribution from inelastic scattering is greatest. The observed differences between the two measurements can be attributed to the presence of plasmon peaks in the EELS spectra which contribute to the raw intensity of both the $^1S_0$ and $^3P_0$ auger lines (see Fig. 5). The background due to the plasmon peaks was not used in the work of Kovalík et al. [19] where only contributions due to inelastically scattered electrons were considered.

Additional peak below the main $^1D_2$ peak in the spectra cannot be completely explained by plasmon losses. This may be due to the presence of shake-up processes as observed in Cu [18]. Recent calculations on the position of this satellite [20] suggest that this peak should appear ≈2 eV closer to the $^1D_2$ than the plasmon peak. We measure the plasmon peak to be at 16 eV energy loss with the position of the satellite at 13 eV, the position of the satellite peak agrees well with that predicted by theory [20].

4. Summary and conclusion

High resolution electron excited KLL AES measurements have been performed on thin self supporting films of Fe, Cu and Ge. They present many of the same problems as AES excited by X-rays. For the elements presented here contribution of both intrinsic ("shake up") and extrinsic (inelastic scattering and plasmon losses) appear in the observed spectra. In all cases it is difficult to separate these contributions.

We have found that application of the often used Shirley background, which is suitable for some investigations, poorly predicts the observed background in Fe and Ge both of which present additional structure in the AES not due to electron losses in their transport to the surface or satellite peaks. The partial intensity analysis (PIA) method of Werner et al. [30,31] offers a more sophisticated technique for describing the complex background by treating the various energy loss mechanisms separately. It is expected that these measurements will provide a new test for the PIA method and help to achieve a thorough understanding of the source of these background.

In this work a different model for the presence of satellite structure in Cu has been presented. We suggest that the satellites observed in Fe , previously identified as plasmon losses are also due to "shake up" processes. In the case of Ge narrow plasmon peaks obscure a satellite, which is visible only after deconvolution of the EELS spectra from the AES.

In general there is good agreement between experiment and theory in all three cases for the relative energies of the Auger lines. Comparison between measured and calculated intensities still remains a problem due to the difficulties in separating and removing contributions from extrinsic processes. Deviations between the intensities presented in this paper and earlier publications [9,18] should be seen as an illustration that the obtained intensity ratio of the multiplets is very sensitive to the data reduction procedure followed, rather than as an indication that results of earlier work are wrong.

For Cu there seems to be a trend that the width of the multiplet is smallest for the $^3P_2$ component, larger for the $^1D_2$ one, and still larger for the $^1S_0$ one. The same trend is seen for the $^3P_2$ and $^1D_2$ lines in Ge, where the width obtained for the $^1S_0$ component is rather unreliable due to its dependence on the deconvolution procedure followed. As life-time broadening of the initial state (the K hole) is identical this observation seems to suggest that additional decay channels are open for the decay of the deeper two-hole final state of the Auger process. For example the decay of the $^1D_2$ state to a $^3P_2$ state coupled to the ejection of a 3d electron is energetically feasible.

It is interesting to compare these KLL Auger of third row elements with the LMM Auger spectra as measured by Kleiman et al. for the fourth row elements Ag [32] and Sn [33]. In both the KLL and LMM experiments satellites are observed. They are attributed to shake effects for the noble metals Cu and Ag and to plasmon excitation for the semiconductors Ge and Sn. The energy separation of the satellites is of comparable magnitude for Cu and Ag. Assuming two satellites for Cu (Model 1) we have a separation from the main line of 11.1 and 7.7 eV for Cu. Kleiman found 13.9 and 5.9 eV for Ag.

In conclusion it is possible to study KLL Auger spectra excited by electrons at an experimental resolution (1 eV) that is better than the intrinsic width of the Auger lines (>4 eV). Quantitative interpretation of the observed spectra, generally in good agreement with Auger spectra obtained by different excitation mechanisms, is surprisingly difficult due to significant influence of extrinsic and intrinsic excitation processes.

Acknowledgements

This work was made possible by a grant of the Australian Research Council. The authors want to thank Anatoli Kheifets for helpful discussions.

References

[1] P. Torelli, M. Sacchi, G. Cautero, M. Cautero, B. Krastanov, P. Lacovig, P. Pittana, R. Sergo, R. Tommasini, A. Fondacaro, F. Offi, G. Paolicelli, G. Stefani, M. Grioni, R. Verbeni, G. Monaco, G. Panaccione, Rev. Sci. Instrum. 76 (2) (2005) 023909.
[2] F.P. Larkins, At. Data Nucl. Data Tables 20 (1977) 311.
[3] M.O. Krause, J. Phys. Chem. Ref. Data 8 (1979) 307.
[4] M. Chen, B. Crasemann, H. Mark, Phys. Rev. A 21 (1980) 442.
[5] M.O. Krause, J.H. Oliver, J. Phys. Chem. Ref. Data 8 (1979) 329.
[6] J.L. Campbell, T. Papp, At. Data Nucl. Data Tables 77 (2001) 1–56.
[7] W. Mehlhorn, R. Albridge, Z. Phys. 175 (1963) 506.
[8] A. Kovalík, A. Inoyatov, A. Novgorodov, V. Brabec, M. Ryšavý, T. Vylov, O. Dragoun, A. Minkova, J. Phys. B: At. Mol. Phys. 20 (1987) 3997.
[9] A. Némethy, L. Kövér, I. Cserny, D. Varga, P. Barna, J. Electron Spectrosc. Relat. Phenom. 82 (1996) 31.
[10] T. Ishii, L. Kövér, Z. Berényi, I. Cserny, H. Ikeno, H. Adachi, W. Drube, J. Electron Spectrosc. Relat. Phenom. 137–140 (2004) 451.
[11] M.H. Chen, B. Crasemann, Phys. Rev. A 8 (1973) 7.
[12] W.N. Asaad, E.H.S. Burhop, Proc. Phys. Soc. 71 (1958) 369.
[13] E. Sokolowoski, C. Nordling, Arkiv for Fysik 14 (1958) 557.
[14] S. Tougaard, J. Kraaer, Phys. Rev. B 43 (1991) 1651.
[15] L. Kövér, Z. Kovács, J. Tóth, I. Cserny, D. Varga, P. Weightman, S. Thurgate, Surf. Sci. 433–435 (1999) 833.
[16] G. Kleimann, S. de Castro, R. Landers, Phys. Rev. B 49 (1994) 9.
[17] I. Cserny, L. Kövér, H. Nakamatsu, T. Mukoyama, Surf. Interface Anal. 30 (2000) 199.
[18] L. Kövér, I. Cserny, J. Tóth, D. Varga, T. Mukoyama, J. Electron Spectrosc. Relat. Phenom. 114–116 (2001) 55.
[19] A. Kovalík, E. Yakushev, D. Filosofov, V. Gorozhankin, T. Vylov, J. Electron Spectrosc. Relat. Phenom. 123 (2002) 65.
[20] Z. Berényi, L. Kövér, S. Tougaard, F. Yubero, J. Tóth, I. Cserny, D. Varga, J. Electron Spectrosc. Relat. Phenom. 135 (2004) 177.
[21] W. Mehlhorn, J. Electron Spectrosc. Relat. Phenom. 93 (1998) 1–15.
[22] G. Beamson, S. Haines, N. Moslemzadeh, P. Tsakiropoulos, J. Watts, P. Weightman, K. Williams, J. Electron Spectrosc. Relat. Phenom. 142 (2005) 151.
[23] M. Vos, G.P. Cornish, E. Weigold, Rev. Sci. Instrum. 71 (2000) 3831.
[24] Y.-K. Kim, J.P. Santos, F. Parente, Phys. Rev. A 62 (2000) 052710.
[25] L. Kövér, S. Tougaard, J. Tóth, L. Daróczi, I. Szabó, G. Langer, M. Menyhárd, Surf. Interface Anal. 31 (2001) 271.
[26] D.A. Shirley, J. Phys. B: At. Mol. Phys. 5 (1972) 4709.
[27] J.E. Castle, A.M. Salvi, Anal. Sci. 17 (2001) 147.
[28] S. Tougaard, Surf. Interface Anal. 11 (1988) 453.
[29] S. Tougaard, Solid State Commun. 61 (1987) 547.
[30] W. Werner, T. Cabela, J. Zemek, P. Jiricek, Surf. Sci. 470 (2001) 325.
[31] W. Werner, L. Kövér, J. Tóth, D. Varga, J. Electron Spectrosc. Relat. Phenom. 122 (2002) 103.
[32] G.G. Kleiman, S.G.C. de Castro, R. Landers, Phys. Rev. B 49 (1994) 2753–2759.
[33] G.G. Kleiman, R. Landers, P.A.P. Nascente, S.G.C. de Castro, Phys. Rev. B 46 (1992) 1970–1974.